Springer

KSME

Journal of Mechanical Science and Technology 28 (12) (2014) 4869~4876
www.springerlink.com/content/1738-494x
DOI 10.1007/s12206-014-1107-1

# Combined rotor fault diagnosis in rotating machinery using empirical mode decomposition †

Sukhjeet Singh and Navin Kumar*

*School of Mechanical Materials and Energy Engineering, Indian Institute of Technology (IIT), Ropar Rupnagar- 140001, Punjab, India*

(Manuscript Received August 2, 2013; Revised June 5, 2014; Accepted September 4, 2014)

**Abstract**

Unbalance, misalignment, partial rub, looseness and bent rotor are one of the most commonly observed faults in rotating machines. These faults cause breakdowns in rotating machinery and create undesired vibrations while operating. In this study, an approach to detect combined fault of unbalance and bent rotors for advance detection of the features of the fault rotors diagnosis is proposed. Empirical mode decomposition (EMD) is used efficiently to decompose the complex vibration signals of rotating machinery into a known number of intrinsic mode functions so that the fault characteristics of the unbalanced and bowed shaft can be examined in the time-frequency Hilbert spectrum. A test bench of Spectra-Quest has been used for performing experiments to illustrate the unbalance and the bent rotor conditions as well as the healthy rotor condition. Analysis of the results shows the usefulness of proposed approach in diagnosing the unbalance and bowed fault of the shaft in rotating machinery.

*Keywords*: Bent rotors; Fault diagnosis; Empirical mode decomposition (EMD); Hilbert-Huang transform (HHT); Unbalance

## 1. Introduction

Mass unbalance is the major source of vibration in rotor systems. Several techniques such as temperature monitoring, acoustic emission, non-destructive testing, visual inspection, motor current signature analysis (MCSA) and vibration based techniques are being used currently for detection of faults. Out of the above techniques, use of vibration based techniques still remains an effective approach. The identification of faults using vibration based techniques such as rotor unbalance [1, 2], rotor bends, cracks rubs [3], misalignment [4], turbines, pumps, compressors, gear boxes [5] and induction motors etc. has been explored immensely. The vibrations can occur due to different reasons like initial deformation or mass unbalance. If the initial deformation in a shaft is also present along with mass unbalance, it gives rise to a synchronous vibration which is different from that obtained with mass unbalance only. It becomes difficult to predict whether the vibration response is because of the mass unbalance or initial permanent deflection or both. Therefore, an in-depth study on the vibration characteristics is very helpful in diagnosing the rotor unbalance to avoid any failure [8].

Vibration analysis techniques have been reported by various researchers in the literature for the diagnosis of faults in rotating machinery [9]. Nicholas [10, 11] conducted first extensive investigation into shaft bow mathematically. They proposed the balancing theory and presented experimental results for the balancing of a flexible rotor with shaft bow. Parkinson et al. [12] described the differences in whirl experienced by a rotating shaft subject to shaft bow and mass unbalance. Shaft bow behavior has also been investigated by many authors [13-15]. Lee [16] has discussed the analytical aspects of rotor dynamics ranging from simple Jeffcott rotor to multi-degree-of-freedom systems.

The influence of bowed rotor on the dynamics of rotor has also been discussed by Ehrich [17]. Rao [18] made an investigation of response of an unbalanced rotor with an initial permanent deflection. Several important observations regarding the use of phase information for detection of the same have been made. Manu and Rao [19] experimentally verified the theoretical results for different case studies given by Rao [18].

It is well known that vibration frequency of rotor unbalance is synchronous with the shaft rotation speed (1X r.p.m.), since the unbalance force rotates at the shaft running speed. Rotor unbalance manifests itself in the frequency domain as a series of harmonics of the shaft running speed, i.e. at 1X rpm, 2X rpm, 3X rpm and 4X rpm. But, the advances in the signal processing techniques have empowered the vibration signal analysis to play an important role in the fault diagnosis. Vibration signal processing analyzes the vibration signal measured at particular locations on the machine, and extracts enough

*Corresponding author. Tel.: +91 1881 242170, Fax.: +91 1881 223395
E-mail address: nkumar@iitrpr.ac.in
† Recommended by Editor Yeon June Kang

information to determine the condition of each of the sub-elements of the machine. The vibration signal contains the information of the oscillatory motion of the machine and its sub-components. Features hidden in the vibration signals can be extracted by the proper selection of appropriate signal processing and hence, assessment of the machine health status can be made [20].

A crack in a shaft, rubbing of stator-rotor arrangement and different faults in a rolling bearing of a machine in operation are some of the examples of signals emerging from the rotating machines. The signals acquired from the rotating machinery are often non-linear and non-stationary. The inability of Fourier transforms to process non-linear and non-stationary signals have been cited by Ref. [21]. Time-frequency analysis techniques, such as the Short-time Fourier transform (STFT) [22] and wavelet transform [23-25] have been used extensively for feature extraction from non-stationary, transient signals. Out of these, wavelet transforms have been reported of analyzing complex vibration signals [26]. But, the limitations of wavelet analysis like energy leakage, interference and distortion at the ends made way for a relatively new technique Hilbert-Huang transform (HHT) [27]. Since its inception, this technique has been exclusively used in various fields viz- biomedical applications, image processing [28], meteorological and atmospheric applications [29], the problems of wind generated ocean wave [30], spectral representation of earthquake data [31], structural health monitoring [32] and speech recognition [33].

Hilbert-Huang transform [21] is based on the principles of empirical mode decomposition (EMD) and Hilbert transform. It extracts the signal characteristics viz- amplitude, instantaneous phase and frequency of vibrations resulting from the intrinsic mode functions (IMFs) of the signal being analyzed and is not constrained by the limitations of time and frequency resolutions as it happens in the case of wavelet analysis. Using this method, any complicated signal can be decomposed into a collection of based on the local time scale features of the signal. The IMFs represent the natural oscillatory mode embedded in the signal [34]. Most of the studies in the recent past have been carried out for diagnosing various faults viz- shaft misalignment [35], bearing faults [36-39, 41], rotor rubbing faults [39], shaft crack faults [40] and gear tooth faults [44] using empirical mode decomposition method (EMD) of the Hilbert-Huang transform technique.

In the present study, an effort has been made to diagnose vibrations for combined unbalance and bowed shaft fault using HHT. The experiments are performed for different bow phase angles viz - 0°, 60°, 120°, 180°, 240° and 300° for the centrally bent shaft and compared with a healthy shaft running at steady speeds. The fault features of centrally bent shaft with different bow angles are successfully detected with the proposed technique. The results reveal the usefulness of time-frequency Hilbert-Huang spectrum for signal decomposition and feature extraction in machine health monitoring applications.

## 2. Theoretical background of Hilbert-Huang transform

Hilbert–Huang transform is based on the principle of empirical mode decomposition and corresponding Hilbert transform. The signals acquired from the vibration analysis of machines are usually non-stationary and nonlinear signals. The drawback of the applicability of the concept of instantaneous frequency to a multi-component signal has been reported by many authors [21, 39, 45, 46]. According to the process defined by Huang et al. [21], a original time series is decomposed in intrinsic mode functions using empirical mode decomposition and then, Hilbert transform is applied to each IMF which leads to obtaining the time-frequency distribution. For understanding the concept of empirical mode decomposition and Hilbert transform, these techniques have been discussed in brief in the following sub-sections:

### *2.1 Empirical mode decomposition method (EMD)*

EMD method is a process in which orthogonal and intrinsic mono components (from an original time series when EMD applied to it) are obtained after a recursive process. The signal is assumed to consist of different intrinsic modes of oscillations. The number of extrema and zero-crossings for each linear or non-linear mode will be same. Any successive zero-crossings will have only one extremum. Each mode should not be dependent on other modes. In this way, each signal could be decomposed into a number of intrinsic mode functions (IMFs) defined by Huang et al. [21]. The IMF's must satisfy two conditions viz – firstly, the number of extrema and the number of zero-crossings must either equal or differ at most by one, secondly the mean value of the envelope defined by local maxima and the envelope defined by the local minima must be zero at any point [21].

The algorithm for obtaining IMF's from a complex signal given by Huang et al. for decomposing any signal x(t) is as follows [21]:

(a) Identify all the local extrema, and then connect all the local maxima by a cubic spline line as the upper envelope.

(b) Repeat the procedure for the local minima to produce the lower envelope. The upper and lower envelopes should cover all the data between them.

(c) The mean of upper and low envelope value is designated as $m_1$, and the difference between the signal x(t) and $m_1$ is the first component, $h_1$, i.e.

$$x(t) - m_1 = h_1 . \tag{1}$$

Ideally, if $h_1$ is an IMF, then $h_1$ is the first component of x(t).

(d) If $h_1$ is not an IMF, $h_1$ is treated as the original signal and repeat (a), (b), (c); then

$$h_1 - m_{11} = h_{11} \tag{2}$$

in which $m_{11}$ is the mean of upper and low envelope value of

$h_1$. After repeated sifting, i.e. up to k times, $h_{1k}$ becomes an IMF, that is

$$h_{1(k-1)} - m_{1k} = h_{1k} \tag{3}$$

then, it is designated as

$$c_1 = h_{1k} \tag{4}$$

the first IMF component from the original data. The shortest period component of the signal is retained in $c_1$.

(e) Separate $c_1$ from x(t), we get

$$r_1 = x(t) - c_1 . \tag{5}$$

$r_1$ is treated as the original data and repeat the above processes, the second IMF component $c_2$ of x(t) could be got. Repeating the process as described above for n times, then n-IMFs of signal x(t) can be achieved got. Then,

$$\begin{aligned} r_1 - c_2 &= r_2 \\ &\vdots \\ r_{(n-1)} - c_n &= r_n . \end{aligned} \tag{6}$$

The decomposition process can be stopped when $r_n$ becomes a monotonic function fromwhich no more IMF can be extracted. By summing up Eqs. (5) and (6), we finally obtain

$$x(t) = \sum_{j=1}^{n} c_j . \tag{7}$$

Residue $r_n$ is the mean trend of x(t). The IMFs $c_1$, $c_2$. . . $c_n$ include different frequency bands ranging from high to low. The frequency components contained in each frequency band are different and they change with the variation of signal x(t), while $r_n$ represents the central tendency of signal x(t).

### *2.2 Hilbert spectrum*

EMD technique decomposes the signal into a number of IMF's and every IMF is a mono-component function. After getting IMFs, Hilbert transform is applied to the original signal to calculate the amplitude and instantaneous frequency.

For one IMF $c_i$ (t) in Eq. (7), we can always have its Hilbert transform as

$$H\left[c_i(t)\right] = \frac{1}{\pi} \int_{-\infty}^{\infty} \frac{c_i(t')}{t - t'} dt' \tag{8}$$

with this definition, we can have an analytic signal as

$$z_i(t) = c_i(t) + jH\left[c_i(t)\right] = a_i(t) e^{j\varnothing_i(t)} \tag{9}$$

where

$$a_i(t) = \sqrt{c_i^2(t) + H^2\left[c_i(t)\right]} \tag{10}$$

$$\varnothing_i(t) = arctan \frac{H\left[c_i(t)\right]}{c_i(t)} . \tag{11}$$

From Eq. (11), we can have the instantaneous frequency as

$$\omega_i(t) = \frac{d\varnothing_i(t)}{dt} . \tag{12}$$

After performing the Hilbert transform to each IMF component, the original signal can be expressed as the real part (RP) in the following form:

$$x(t) = RP \sum_{i=1}^{n} a_i(t) e^{j\varnothing_i(t)} = a_i(t) e^{j\int \omega_i(t) dt} . \tag{13}$$

Here, we left out the residue rn on purpose, for it is either a monotonic function or a constant. Eq. (13) gives both amplitude and frequency of each component as functions of time. This frequency-time distribution of the amplitude is designated as the Hilbert spectrum H (ω, t):

$$H(\omega, t) = RP \sum_{i=1}^{n} = a_i(t) e^{j\int \omega_i(t) dt} . \tag{14}$$

Since the IMFs have well - behaved Hilbert transforms, the corresponding instantaneous frequencies are calculated. The local energy and the instantaneous frequency derived from the IMFs give us a full energy-frequency-time distribution of the data and such a representation is designated as the Hilbert spectrum.

## 3. Experimental setup

The experimental setup consists of a machinery fault simulator (MFS) test bench manufactured by Spectra Quest®, Inc. The schematic of the MFS is shown in Fig. 1. The configuration of the setup consists of a slotted disc (aluminium) mounted on a 19.05 mm dia shaft (cold rolled steel), and the shaft is supported on two identical roller bearings. The shaft is attached to a torsionally stiff spring coupling that is driven by a three phase 3/4 HP induction motor. A variable frequency drive (VFD) has been attached with the induction motor so as to adjust the motor speed which can be increased or decreased in the range from 0 to 4500 rpm. Reverse dial gauge method is used to align the shaft with the motor end shaft. A pair of proximity probes are mounted radially (in horizontal and vertical directions) on the rotor system with an attachment. Two shafts, one healthy (HS) and one centrally bent shaft (CBS)

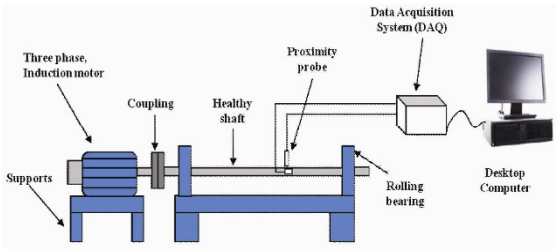


Fig. 1. Line diagram of the experimental setup.

with a bend of 200 microns are used to simulate the different shaft unbalance conditions.

For simulating unbalance, the holes in the disc can be loaded with nuts and bolts of predetermined weight of 9 g. First, the experiments are performed for healthy shafts with/without disk along with one unbalance. Then, experiments are performed for different bow phase angles viz - 0°, 60°, 120°, 180°, 240° and 300° for the centrally bent shaft running at steady speeds. The bending natural frequency ($\omega_n/2$) of the shafts is 59.5 Hz. The rotational speed considered for this study is one half of the first bending natural frequency 29.9 Hz for the shafts.

## 4. Results and discussion

The difficulty in extracting the fault information from the complex non-stationary and non-linear vibration signal has led to the development of specialized techniques apart from traditional approaches. Out of these techniques, Hilbert-Huang transform technique has been successfully used by researchers in the literature for diagnosing various faults viz- shaft misalignment [35], gear tooth faults [36] and bearing faults [41] and because of its wide applicability. Fast Fourier transform (FFT) and Hilbert-Huang transform (HHT) are based on different approaches [47]. FFT assumes the linearity and stationarity of the data i.e. it can only process linear data. It is also dependent on the globally defined orthogonal basis states, whereas, HHT has an edge over FFT in the sense that it can process non-linear and non-stationary data. In this transform, global basis states must be replaced with adaptive, locally determined ones. Also, the resulting basis states are not required to be strictly orthogonal. The traditional way of observing signals is to view them in time domain. The wave form of a healthy shaft (unbalanced disk) running at $\omega_n/2$ acquired with a proximity probe (PP) has been shown in Fig. 2(a). Similarly Figs. 2(b)-(g) show the waveforms of a CBS with one unbalance running at $\omega_n/2$ at different bow phase angles (BP) varying from 0°-300° with increments of 60° respectively. In Fig. 2(b), as the bow phase angle is 0° which means that the unbalance and the bow are on the same side, so the vibration amplitude of such a rotor should be higher than the healthy rotor running with same conditions [18]. The vibration amplitude of CBS with BP 0° is 0.6428 mils, whereas for HS with disk and unbalance it is 0.3088 mils.

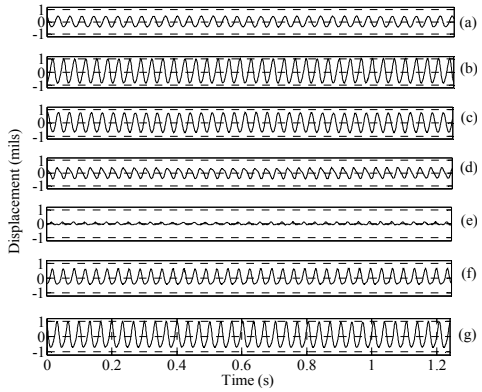


Fig. 2. Displacement waveform of the healthy shaft (unbalanced disk at $\omega_n/2$) and centrally bent shaft (unbalanced disk at $\omega_n/2$) at different bow phase angles respectively.

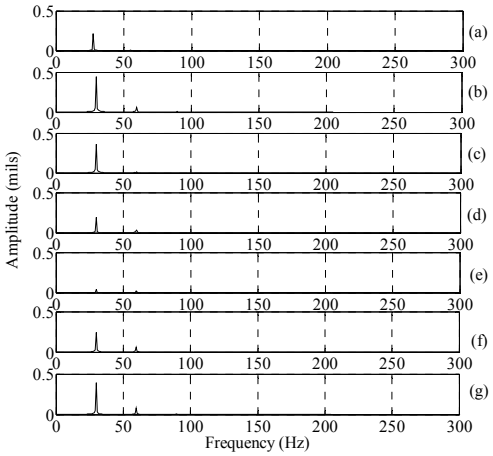


Fig. 3. Spectrum of the healthy shaft (unbalanced disk at $\omega_n/2$) and centrally bent shaft (unbalanced disk at $\omega_n/2$) at different bow phase angles.

With BP angle 60° for a CBS, the amplitude is 0.5219 mils and for BP angle 120°, the magnitude is 0.2821 mils. In Fig. 2(e), the amplitude reaches to a lower value (0.0657 mils) when the BP is 180°, which means the bow and the unbalance are opposite to each other. With further changing of the BP angle with CBS running at $\omega_n/2$ to 240° (0.36828 mils) and 300° (0.5837 mils) leads to an increase in the amplitude of the vibrations, but less than the maximum amplitude attained when the BP was 0°. Preliminary investigation for the faults in the acquired signals has been done using fast Fourier transforms (FFT). Figs. 3(a)-(g) shows the FFT spectrum of the HS and CBS (at different BP angles) with unbalance running at $\omega_n/2$ respectively. For the subsequent vibration spectra, the analysis bandwidth has been limited to 300 Hz. From the Fig. 3, it is seen that the vibration frequency of rotor unbalance is synchronous, i.e., one time the shaft rotation speed (1X r.p.m.). As the BP angle is changed from 0° to 300° for the CBS, a variation in the vibration amplitude is observed. The magnitude of the CBS at BP 0° is higher than the amplitude obtained at other BP angles and the healthy shaft.

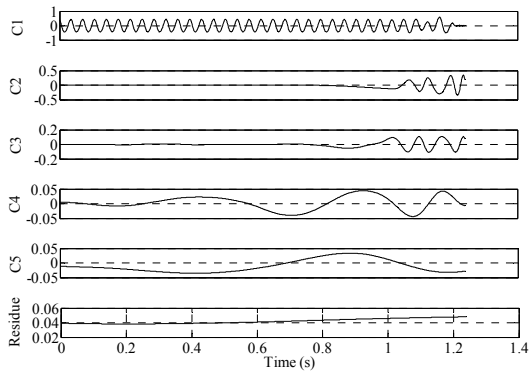


Fig. 4. IMF's of the healthy shaft.

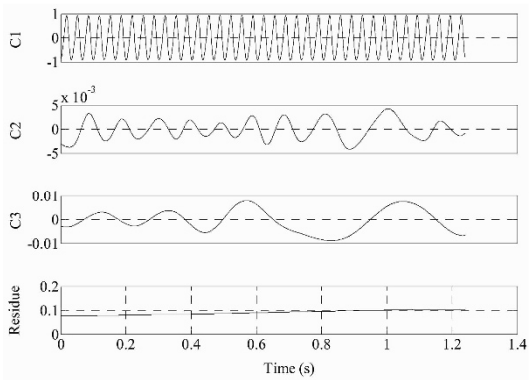


Fig. 5. IMF's of centrally bent shaft (unbalanced disk) at bow phase angle 0°.

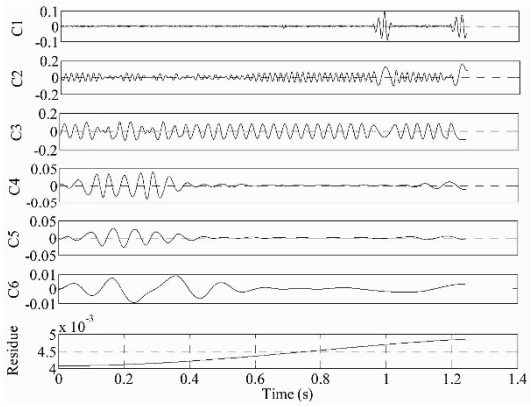


Fig. 6. IMF's of centrally bent shaft (unbalanced disk) at bow phase angle 180°.

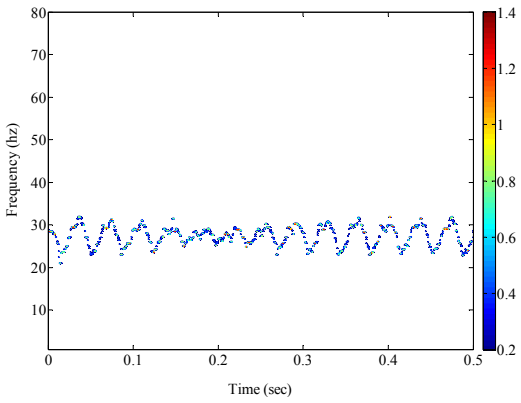


Fig. 7. Contour plot of the healthy shaft.

At 180° BP condition, a decrease in the amplitude of the vibration is seen. FFT can diagnose the unbalance, but could not diagnose the effect of a bowed shaft along with an unbalance present in the rotor. Therefore, HHT technique has been applied to data acquired for healthy and centrally bent shafts for making further investigations.

From the Sec. 2, we need to efficiently decompose the complicated vibration signals of rotating machinery into a finite number of intrinsic mode functions (IMFs) in order to study the fault characteristics in the time-frequency Hilbert spectrum. The IMF's of vibration signals for three cases, viz- HS (with unbalanced disk) and CBS (with unbalanced disk with BP angle 0° and 180° running at $\omega_n/2$ have been shown in Figs. 4-6. The IMF's in three cases have been shown in time domain showing variation of amplitude in each frequency range with time. The IMF's contain frequencies in the decreasing order, with the first IMF (C1) indicating the maximum rate of change of amplitude and the last IMF known as residue indicates the variations with the slowest rate. The variation in the number of the IMF's generated for the various conditions is because of the self-adaptive nature of the EMD process.

For healthy shaft, only six IMF's have been generated whereas for centrally bent shaft the IMF's generated are varying (four for CBS with BP at 0° and nine for CBS with BP at 180°). The first IMF of the Figs. 4 and 5 can be seen to be similar to the original signal, as it shows the highest frequencies contained in the signal. Third IMF in the case of the CBS with unbalanced disk at 180°, Fig. 6 shows similarity to the original signal. Since IMF's show presence of frequencies but do not reveal much about the fault and the extent of fault. The wiggle phenomena seen in the intrinsic mode functions C2 and C3 in Fig. 4 at the end of analyzing time, and C4, C5 and C6 in Fig. 5 in the beginning is the mode mixing problem of empirical mode decomposition (EMD). It is one of the limitations of EMD. Wiggle is the under shoot or overshoot during the sifting process and it corrupts the decomposition. The mode mixing problem can be taken care by using the ensemble empirical mode decomposition [35]. It is clear from the Fig. 6 that the IMF's with order frequencies experience largest variation when the bow phase angle changes to 180°. Fig. 7 shows the time-frequency Hilbert Huang spectrum of all the cases of the vibration data respectively within the frequency band of the shaft rotating speed.

The HHT spectrum of the healthy shaft (with unbalanced disk at $\omega_n/2$) in Fig. 7 shows that the mono component corresponding to $\omega_n/2$ experiences a variation in the frequency. It shows that the frequency of the major concentrated vibration

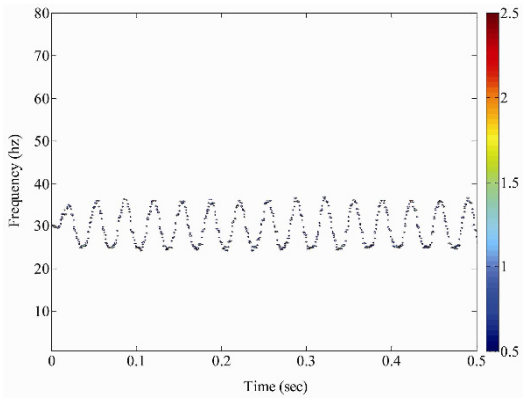


Fig. 8. Contour plot of the centrally bent shaft (unbalanced disk) at bow phase angle of 0°.

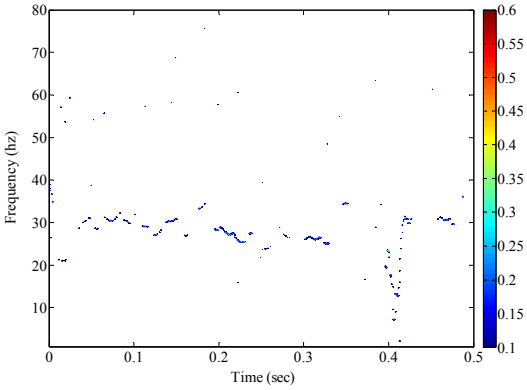


Fig. 9. Contour plot of the centrally bent shaft (unbalanced disk) at bow phase angle of 180°.

energy fluctuates with a mean frequency of $\omega_n/2$.

This variation in the frequency phenomenon in the HHT spectrum is known as intra-wave frequency modulation and it represents nonlinear behavior [35].

The HHT spectrum for the centrally bent shaft with unbalanced disc and the bow phase angle 0° shows an increase in the frequency band of the intra-wave frequency modulation, Fig. 8. This result is similar to the Fig. 2(b) in which the amplitude of the centrally bent shaft with unbalanced disc and the bow phase angle 0° vibration signal is more than the healthy shaft running at same conditions [18].

It is known that at bow phase angle 180°, bow and the unbalance are opposite to each other and they try to balance out each other resulting in the lower amplitude of the vibration refer Figs. 2(e) and 3(e). The HHT spectrum for this case shown in Fig. 10 reveals that in order to balance the shaft, the mean amplitude of frequency band of the intra-wave frequency modulation becomes far smaller in comparison to the mean amplitude of healthy shaft without disk and centrally bent shaft with unbalanced disc.

## 5. Conclusions

In this paper, combined unbalance and bowed shaft faults have been investigated using Fourier transform and Hilbert-Huang transform. The vibration response of the healthy shaft and the faulty shafts has been compared using FFT. In the FFT analysis, it is difficult to diagnose the combined fault of unbalance and bow phase angle, whereas by using HHT analysis, the fault feature can be diagnosed in the form of increase in the intra-wave frequency band. With the IMF's generated using EMD and contour plots using Hilbert-Huang technique, one can recognize the frequency components that exist in the system and one can have a more clarity about its information contained in the vibration signal in comparison to the other existing signal processing techniques. It is seen from the results that for the centrally bent shaft with unbalanced disc and the bow phase angle 0° shows an increase in the frequency band of the intra-wave frequency modulation, whereas for the same case with bow phase angle of 180°, the a decrease in the frequency band has been noticed. Results indicate that the mono components corresponding to the running speed experience variation in the frequency under different shaft faults in comparison to the healthy shafts.

## References

[1] A. S. Sekhar, Identification of unbalance and crack acting simultaneously in a rotor system: Modal expansion versus reduced basis dynamic expansion, *Journal of Vibration and Control*, 11 (9) (2005) 1125-1145.

[2] Y. Peng, M. Dong and M. J. Zuo, Current status of machine prognostics in condition-based maintenance: a review, *The International Journal of Advanced Manufacturing Technology*, 50 (1-4) (2010) 297-313.

[3] N. Bachschmid, P. Pennacchi and A. Vania, Thermally induced vibrations due to rub in real rotors, *Journal of Sound and Vibration*, 299 (4-5) (2007) 683-719.

[4] A. R. Mohanty, A. S. Sekhar and S. Prabhakar, Vibration analysis of a misaligned rotor-coupling-bearing system passing through the critical speed, *Proceedings of the Institution of Mechanical Engineers, Part C: Journal of Mechanical Engineering Science*, 215 (12) (2001) 1417-1428.

[5] Z. Su, Y. Zhang, M. Jia, F. Xu and J. Hu, Gear fault identification and classification of singular value decomposition based on Hilbert-Huang transform, *Journal of Mechanical Science and Technology*, 25 (2) (2011) 267-272.

[6] J. K. Dutt and B. C. Nakra, Stability of rotor systems with viscoelastic supports, *Journal of Sound and Vibration*, 153 (1) (1992) 89-96.

[7] G. Genta and F. De Bona, Unbalance response of rotors: A modal approach with some extensions to damped natural systems, *Journal of Sound and Vibration*, 140 (1) (1990) 129-153.

[8] S. Edwards, A. W. Lees and M. I. Friswell. *The identification of a rotor bend from vibration measurements, Society for Experimental Mechanics, IMAC XVI - 16th International Modal Analysis Conference, 1998* (1998).

[9] S. Edwards, A. Lees and M. Friswell, Fault diagnosis of

rotating machinery, *Shock and Vibration Digest*, 30 (1998) 4-13.

[10] J. C. Nicholas, E. J. Gunter and P. E. Allaire, Effect of residual shaft bow on unbalance response and balancing of a single mass flexible rotor Part I- Unbalance response, *J Eng Power Trans ASME*, 98 Ser A (1976) 182-189.

[11] J. C. Nicholas, E. J. Gunter and P. E. Allaire, Effect of residual shaft bow on unbalance response and balancing of a single mass flexible rotor Part II -Balancing, *J Eng Power Trans ASME*, 98 Ser A (1976) 171-181.

[12] A. G. Parkinson, M. S. Darlow and A. J. Smalley, Balancing flexible rotating shafts with an initial bend, *AIAA Journal*, 22 (5) (1984) 683-689.

[13] W. L. Meacham, P. B. Talbert, H. D. Nelson and N. K. Cooperrider, Complex modal balancing of flexible rotors including residual bow, *Journal of Propulsion and Power*, 4 (3) (1988) 245-251.

[14] R. D. Flack, J. H. Rooke, J. R. Bielk and E. J. Gunter, Comparison of the unbalance responses of Jeffcott rotors with shaft bow and shaft runout, *Journal of Mechanical Design*, 104 (1982) 318-328.

[15] D. Salamone and E. Gunter, Synchronous unbalance response of an overhung rotor with disk skew, *Journal of Engineering for Power*, 102 (1980) 749-755.

[16] C. W. Lee, *Vibration analysis of rotors,* Kluwer Academic, Dordrecht (1993).

[17] F. F. Ehrich, *Handbook of rotor dynamics,* McGraw - Hill Inc, New York (1992).

[18] J. S. Rao, A note on Jeffcott warped rotor, *Mechanism and Machine Theory*, 36 (5) (2001) 563-575.

[19] J. S. Rao and M. Sharma, Dynamic analysis of bowed rotors, *Advances in Vibration Engineering*, 2 (2) (2003) 1-14.

[20] Y. Ruqiang and R. X. Gao, Hilbert–huang transform-based vibration signal analysis for machine health monitoring, *Instrumentation and Measurement, IEEE Transactions on*, 55 (6) (2006) 2320-2329.

[21] N. E. Huang, Z. Shen, S. R. Long, M. C. Wu, H. H. Shih, Q. Zheng, N. C. Yen, C. C. Tung and H. H. Liu, The empirical mode decomposition and the Hilbert spectrum for nonlinear and non-stationary time series analysis, *Proceedings of the Royal Society A: Mathematical, Physical and Engineering Sciences*, 454 (1971) (1998) 903-995.

[22] L. Satish, Short-time Fourier and wavelet transforms for fault detection in power transformers during impulse tests, *IEE Proceedings: Science, Measurement and Technology*, 145 (2) (1998) 77-84.

[23] K. Mori, N. Kasashima, T. Yoshioka and Y. Ueno, Prediction of spalling on a ball bearing by applying the discrete wavelet transform to vibration signals, *Wear*, 195 (1-2) (1996) 162-168.

[24] W. Changting and R. X. Gao, Wavelet transform with spectral post-processing for enhanced feature extraction [machine condition monitoring], *Instrumentation and Measurement, IEEE Transactions on*, 52 (4) (2003) 1296-1301.

[25] R. Yan and R. X. Gao, An efficient approach to machine health diagnosis based on harmonic wavelet packet transform, *Robotics and Computer-Integrated Manufacturing*, 21 (4-5) (2005) 291-301.

[26] P. W. Tse, W.-X. Yang and H. Tam, Machine fault diagnosis through an effective exact wavelet analysis, *Journal of Sound and Vibration*, 277 (4) (2004) 1005-1024.

[27] N. E. Huang, M.-L.C. Wu, S. R. Long, S. S. P. Shen, W. Qu, P. Gloersen and K. L. Fan, A confidence limit for the empirical mode decomposition and Hilbert spectral analysis, *Proceedings of the Royal Society of London. Series A: Mathematical, Physical and Engineering Sciences*, 459 (2037) (2003) 2317-2345.

[28] H. Hariharan, A. Gribok, M. A. Abidi and A. Koschan, Image fusion and enhancement via empirical mode decomposition, *Journal of Pattern Recognition Research*, 1 (1) (2006) 16-32.

[29] J. I. Salisbury and M. Wimbush, Using modern time series analysis techniques to predict ENSO events from the SOI time series, *Nonlinear Processes in Geophysics*, 9 (3/4) (2002) 341-345.

[30] P. A. Hwang, N. E. Huang and D. W. Wang, A note on analyzing nonlinear and nonstationary ocean wave data, *Applied Ocean Research*, 25 (4) (2003) 187-193.

[31] N. E. Huang, A new spectral representation of earthquake data: Hilbert spectral analysis of station, *Bulletin of the Seismological Society of America,* 91 (5) (1991) 1310-1338.

[32] S. T. Quek, P. S. Tua and Q. Wang, Detecting anomalies in beams and plate based on the Hilbert–Huang transform of real signals, *Smart Materials and Structures*, 12 (3) (2003) 447.

[33] H. Huang and J. Pan, Speech pitch determination based on Hilbert-Huang transform, *Signal Processing*, 86 (4) (2006) 792-803.

[34] Q. Gao, C. Duan, H. Fan and Q. Meng, Rotating machine fault diagnosis using empirical mode decomposition, *Mechanical Systems and Signal Processing*, 22 (5) (2008) 1072-1081.

[35] T. Y. Wu and Y. L. Chung, Misalignment diagnosis of rotating machinery through vibration analysis via the hybrid EEMD and EMD approach, *Smart Materials and Structures*, 18 (9) (2009) 095004.

[36] J. Cheng, D. Yu, J. Tang and Y. Yang, Application of frequency family separation method based upon EMD and local Hilbert energy spectrum method to gear fault diagnosis, *Mechanism and Machine Theory*, 43 (6) (2008) 712-723.

[37] H. Li, Y. Zhang and H. Zheng, Hilbert-Huang transform and marginal spectrum for detection and diagnosis of localized defects in roller bearings, *Journal of Mechanical Science and Technology*, 23 (2) (2010) 291-301.

[38] H. Dong, K. Qi, X. Chen, Y. Zi, Z. He and B. Li, Sifting process of EMD and its application in rolling element bearing fault diagnosis, *Journal of mechanical science and technology*, 23 (8) (2009) 2000-2007.

[39] T. H. Patel and A. K. Darpe, Study of coast-up vibration response for rub detection, *Mechanism and Machine Theory*, 44 (8) (2009) 1570-1579.

[40] B. Ramesh, S. Srikanth and A.S. Sekhar, Hilbert–Huang transform for detection and monitoring of crack in a transient rotor, *Mechanical Systems and Signal Processing*, 22 (4) (2008) 905-914.
[41] C. Junsheng, Y. Dejie and Y. Yu, A fault diagnosis approach for roller bearings based on EMD method and AR model, *Mechanical Systems and Signal Processing*, 20 (2) (2006) 350-362.
[42] X. Fan and M. J. Zuo, Gearbox fault detection using Hilbert and wavelet packet transform, *Mechanical Systems and Signal Processing*, 20 (4) (2006) 966-982.
[43] K. Aharamuthu and E. P. Ayyasamy, Application of discrete wavelet transform and Zhao-Atlas-Marks transforms in non stationary gear fault diagnosis, *Journal of Mechanical Science and Technology*, 27 (3) (2013) 641-647.
[44] H. Li, Y. Zhang and H. Zheng, Wear detection in gear system using Hilbert-Huang transform, *Journal of Mechanical Science and Technology*, 20 (11) (2006) 1781-1789.
[45] B. Yang and C. S. Suh, Interpretation of crack-induced rotor non-linear response using instantaneous frequency, *Mechanical Systems and Signal Processing*, 18 (3) (2004) 491-513.
[46] B. Boashash, Estimating and interpreting the instantaneous frequency of a signal. I. Fundamentals, *Proceedings of the IEEE*, 80 (4) (1992) 520-538.
[47] D. Donnelly, The fast Fourier and Hilbert-Huang transforms: a comparison. in Computational Engineering in Systems Applications, *IMACS Multi conference on*, IEEE (2006).

**Navin Kumar** is an Assistant Professor in the School of Mechanical Materials and Energy Engineering at Indian Institute of Technology (IIT), Ropar, India. Prior to joining IIT Ropar, he was working as a Research Scientist at Stevens Institute of Technology, New Jersey, USA. He did Masters in Mechanical Engineering from Indian Institute of Technology, Kharagpur, India and Ph.D. (Mechanical Engineering). Dr. Navin Kumar's research interests are related to smart structures and materials, fault diagnosis and condition monitoring.

**Sukhjeet Singh** is a Research Scholar in the School of Mechanical Materials and Energy Engineering at Indian Institute of Technology, Ropar, India. He received his Bachelor's (Mech Engg) and Master's degree (Machine design) from the Punjab Technical University, Jalandhar, Punjab, India. His research interests include experimental aspects of vibration analysis, rotor dynamics, signal processing and machine learning techniques.